Phosphorescence Lifetime Analysis with a Quadratic Programming Algorithm for Determining Quencher Distributions in Heterogeneous Systems

Sergei A. Vinogradov and David F. Wilson
Department of Biochemistry and Biophysics, School of Medicine, University of Pennsylvania, Philadelphia, Pennsylvania 19104 USA

ABSTRACT A new method for analysis of phosphorescence lifetime distributions in heterogeneous systems has been developed. This method is based on decomposition of the data vector to a linearly independent set of exponentials and uses quadratic programming principles for χ^2 minimization. Solution of the resulting algorithm requires a finite number of calculations (it is not iterative) and is computationally fast and robust. The algorithm has been tested on various simulated decays and for analysis of phosphorescence measurements of experimental systems with descrete distributions of lifetimes. Critical analysis of the effect of signal-to-noise on the resolving capability of the algorithm is presented. This technique is recommended for resolution of the distributions of quencher concentration in heterogeneous samples, of which oxygen distributions in tissue is an important example. Phosphors of practical importance for biological oxygen measurements: Pd-*meso*-tetra (4-carboxyphenyl) porphyrin (PdTCPP) and Pd-*meso*-porphyrin (PdMP) have been used to provide experimental test of the algorithm.

INTRODUCTION

Our research group is using the oxygen-dependent quenching of phosphorescence to measure oxygen in biological systems (Vanderkooi et al., 1987; Wilson et al., 1988; Rumsey et al., 1988; Robiolio et al., 1989; Pawlowski and Wilson, 1992; Shonat et al., 1992; Wilson and Vinogradov, 1993). This is a noninvasive optical technique that has been successfully used for both in vitro and in vivo measurements of oxygen pressure. The physical basis of the technique is that when the phosphorescent probes are in the excited triplet state they can either emit light or transfer the energy to other molecules and return to the ground state without radiation (Scheme 1).Thus,

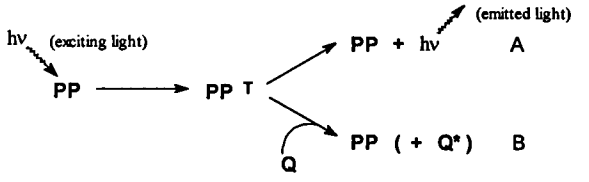

SCHEME 1

excited phosphor PP^T decays by two major competing processes: radiative decay (A) and nonradiative energy transfer to quencher molecule Q (B) (Eq. 1).

$$\frac{d[PP^T]}{dt} = -k_1[PP^T] - k_q[PP^T][Q] \qquad (1)$$

Generally, we can assume that quenching agent is present in the system in large excess compared with the excited triplet state molecules. In this case, as long as process B is a simple bimolecular reaction (e.g., the rate-limiting step is not delivery of the quencher or formation of a chemical adduct between the quencher and the probe molecule), the variables in Eq. 1 can be separated and subsequent integration gives

$$[PP^T] = [PP_0^T] \cdot \exp(-(k_1 + k_q[Q]) \cdot t), \qquad (2)$$

where $[PP_0^T]$ denotes concentration of triplet state molecules immediately after the flash of excitation light. The intensity of emitted light is proportional to concentration of triplet state molecules, and Eq. 2 can be rewritten in the form

$$I = I_0 \cdot \exp\left(-\frac{t}{\tau}\right), \qquad (3)$$

where

$$\frac{1}{\tau} = \frac{1}{\tau_0} + k_q[Q]. \qquad (4)$$

Here $1/\tau_0 = k_1$ is the characteristic lifetime of the phosphorescence decay in the absence of quencher (the second term in Eq. 1 is equal to zero), whereas k_q is related to the frequency of collision between triplet state probe molecules and quencher and is a second order rate constant. These two parameters are characteristic of the probe and its environment and thus need to be measured as part of the calibration. Equation 4, the so called Stern-Volmer relationship, allows calculation of the concentration of quencher from the measured phosphorescence lifetime and the measured values of k_q and τ_0.

To obtain the kinetic parameters of the system, such as the characteristic lifetimes, measurements of the phosphorescence decay have to be subject to appropriate numerical analysis. Fitting of an acquired data-vector with a single exponential curve (Eq. 3) automatically assumes homogeneity of the sample. This situation is practically realized when one measures phosphorescence from a cuvette with homogenous

Received for publication 5 July 1994 and in final form 9 August 1994.
Address reprint requests to Dr. David F. Wilson, Department of Biochemistry/Biophysics, University of Pennsylvania, Philadelphia, PA 19104. Tel.: 215-898-6382; Fax: 215-898-4217.
© 1994 by the Biophysical Society
0006-3495/94/11/2048/12 $2.00

solution of probe at a given quencher concentration. In this case, all of the "elementary volumes" of the sample are characterized by the same decay constant and their sum is also a single exponential. Thus, a simple weighted linear least-square fitting can be applied to the logarithm of data vector. However, it should be pointed out that the Stern-Volmer relationship holds only when the concentrations of quencher are greater than the concentration of the probe in the excited state. There can be significant deviations from this relationship if measurements are made where the quencher concentration approaches that of the excited state molecules. Deviation from Stern-Volmer behavior also occurs when the assumption of pure dynamic quenching is not valid (Carraway et al., 1991).

Samples with microheterogeneity, on the other hand, present much more complex phosphorescence decays made up of many different exponentials and, therefore, the data vector should be analyzed differently (Ware, 1991). A function containing several exponential terms (usually no more then 3–4, Eq. 3) can be used if one assumes that sample has a few discrete "independent phosphorescence sources" or only few discrete quencher concentrations in the volume.

$$I = I_1 \cdot \exp(-t/\tau_1) + I_2 \cdot \exp(-t/\tau_2) + \cdots \quad (5)$$

A possible practical realization of this case is a solution containing several phosphorescent probes with different τ_o and k_q values. Nonlinear fitting by varying both I_i and τ_i leads to its optimal values, but the number of components in the probe function should be chosen in advance. In other words, a priori knowledge of certain discrete decay components is required. Moreover, choosing the wrong number of exponential terms can result in calculation of physically meaningless values. A two or three exponential decay can be satisfactory fitted with sum of 5–6 exponentials and, conversely, three or four exponential functions can adequately fit complex sets of decays (James and Ware, 1985). Thus, evaluation of quencher concentration in heterogeneous samples such as luminescent metal complexes adsorbed on silica surface (Carraway et al., 1991a) or incorporated into the polymer films (Sacksteder et al., 1993) has been attempted by fitting to decay of 3–4 discrete exponentials and using the weighted average lifetime (Carraway et al., 1991b).

Heterogeneous luminescence systems, however, often can be described as a sum of a very large number of individual lumophores, and resulting response is, in fact, convolution of a broad distribution of independent decays. In biological systems such as animal tissue with phosphor in solution in the blood, heterogeneity arises from the wide range of oxygen concentrations in the sampled volume of tissue. After being exposed to a flash of exciting light, an area of tissue is, in fact, a very large number of tiny light emitters, each with a phosphorescence lifetime characteristic of the oxygen pressure in its local environment. Thus, deconvolution techniques that do not introduce bias concerning the number of decays are needed for reconstruction of the distribution of lifetimes. In blood, oxygen pressure ranges from that in the arterioles to below that in the veins and, depending on the physiological conditions, this means from 0 to about 100 Torr. For the conditions of typical biological experiments (see, for example, Rumsey et al., 1988), the concentration of phosphorescent probe is about 5 μmol/l. Approximate calculations based on a quantum yield of 0.1–0.4 for Pd-porphyrin phosphorescence (Eastwood and Gouterman, 1970), extinction coefficients of about 25,000 mol/cm^{-1}, and intensities and lifetimes of typically used flash lamps give concentrations of excited phosphor of about 0.2–5 $\times$ 10^{-9} M. This is three to four orders of magnitude lower than lowest oxygen concentration to be measured. Thus, the Stern-Volmer equation is appropriate to use for conversion from lifetime to oxygen concentration domains.

Recently, powerful iterative algorithms called the Exponential Series Method (ESM) and the Maximum Entropy Method (MEM) have been applied to the analysis of fluorescence decay data collected from heterogeneous samples (Ware et al., 1973; James and Ware, 1986; Livesey, 1987; Siemiarczuk and Ware, 1989; Ware, 1991; Peckan, 1992; Gehlen and Shryver, 1993; Siemiarczuk, 1993). An approach called Expectation Maximization has also been tested on computer-simulated multiexponential decays (Stanley et al., 1993). Comparison of the first two methods indicated that they are almost equally capable of recovering the underlying lifetime distributions (Siemiarczuk et al., 1990). ESM was suggested as the method of choice because of faster execution and lower requirements for the computer resources. It has been pointed out (Ware et al., 1973) that this analytical technique could be applied to the phosphorescence decays as well. However, the authors considered that the poor accuracy of phosphorescence data compared with those for fluorescence measured by Single Photon Counters made ESM analysis of questionable applicability to interpretation of phosphorescence decays.

The accuracy of time-resolved phosphorescence measurements has been significantly improved in recent years (Pawlowski and Wilson, 1992). Utilization of well designed flash illuminators in combination with sensitive photomultipliers has allowed substantial increase in the signal-to-noise ratio of acquired data, and fast 12 bit A/D converters allow the data to be digitized with sufficient accuracy for analysis using multiexponential deconvolution techniques. The improved signal-to-noise for each measurement, combined with the use of rapid repetitive summation and averaging of the measured phosphorescence decays, has resulted in acquisition of data with very low noise.

In the present paper, we report a deconvolution method that utilizes the same algebraic methodology as in ESM, but approaches function minimization through quadratic programming principles. Software has been written and tested on a number of simulated decay curves with various distributions of exponential decays and noise levels. The program was then utilized in the analysis of the data collected from solutions of phosphors to determine its ability to resolve phosphorescence decays separated in lifetime space. Finally, the method has been applied to evaluation of the accuracy of

the k_q and τ_o values, determined by conventional single exponential fitting, of the important phosphors: Pd-*meso*-tetra (4-carboxyphenyl) porphyrin (PdTCPP), and Pd-*meso*-porphyrin, bound to the large protein molecule Bovine Serum Albumin; these phosphorescent probes are widely used in biological experiments. To our knowledge, this approach has not been previously applied to analysis of the distribution of phosphorescence lifetimes.

THEORY

If a data vector $I(t)$ is a convolution of an infinite numbers of exponential decays, characterized by τs, spaced in a defined range, and $g(\tau)$ is signal spectrum (a function describing the distribution), the transformation $g(\tau) \Rightarrow I(t)$ is a Laplace transform (L), and it is presented by the integral (Eq. 6) over the exponential kernel.

$$I(t) \overset{L}{=} \int_0^\infty g(\tau) \cdot \exp\left(-\frac{t}{\tau}\right) d\tau \qquad (6)$$

Therefore, recovery of the distribution (finding $g(\tau)$ from measured $I(t)$) includes inversion of Laplace transform (L^{-1}), which belongs to the class of ill-posed problems (McWhirter and Pike, 1978). Several deconvolution methods based on analytical inversion of the Laplace transform have been proposed in the past (Gardner et al., 1959; Provencher, 1976a, 1976b); however, none of them has become a method of extensive practical use.

The method presented here utilizes algebraic methodology, namely, decomposition of a vector (data vector from the experiment) into a linearly independent basic set of single exponentials. Although this formalism is similar to that used in ESM and other techniques, we will briefly describe the main considerations. Assuming that characteristic lifetimes τ_k of the exponentials are fixed and only the linear coefficients b_k vary, the probe function for the decay has a linear form (Eq. 7).

$$I(t) = \sum_k^N b_k \cdot \exp\left(-\frac{t}{\tau_k}\right) \qquad (7)$$

The question of including optical pumping source function and instrument response function to the model have been discussed previously (Ware et al., 1973). This is necessary when the luminescence decay is significantly distorted by the excitation pulse and the response of the measuring system. Such a situation occurs, for instance, in fluorescence lifetime measurements, when characteristic lifetimes of the decays are comparable with average duration of the excitation pulse. One of the advantages of phosphorescent systems is their relatively slow decay kinetics. The measured lifetimes often lie in the range of 20 μs to 1 ms, whereas suitable excitation lamps are available with flash durations of less than 5 μs. Thus, the contribution of the flash can be readily removed during data analysis. Another advantage is that light emitted by phosphorescence probe is usually shifted to substantially longer (10–100 nm) wavelengths than the absorption (excitation) wavelengths. Use of high selectivity optical filters, such as multilayer interference filters, allows almost total exclusion of excitation light from the detector. Thus, for measurements of phosphorescence it is generally not necessary to be concerned about convolution of the excitation pulse and instrument response functions at the stage of design matrix computation. As it will be shown below, analysis of the decays collected from samples that do not contain phosphor shows the validity of such an approximation.

The family of exponentials with lifetimes uniformly spaced between τ_{min} and τ_{max} in τ-space or between $1/\tau_{max}$ and $1/\tau_{min}$ in reciprocal τ-space was chosen as a basis for our deconvolutions, but in principal any set of linearly independent functions, such as sets of polynomials or trigonometric functions, can be used (Ware et al., 1973). When choosing exponentials, certain physical significance can be attributed to the shape of the recovered distribution. The number of functions used in the solution is limited by computer memory and time of computation, whereas the data vector is represented by a continuous sum of decays. Therefore, decomposition has been designed to find the best approximate solution, and χ^2 criteria have been chosen for determination of goodness of fit. Provencher (1982a) pointed out that choosing a unique solution from the large set of solutions that satisfy data within experimental error is potentially difficult when one employs ordinary χ^2 criteria to evaluate agreement between data and recovered parameters. This is because of the presence of noise in the measured decays. More general approaches such as Regularized Least Squares (Provencher, 1982a, b) and General Cross-Validation (Stanley et al., 1993) incorporate so called *regularizers* to achieve stability of the solution at higher noise levels. As it will be shown below, in our case experimentally obtained signal-to-noise ratios (SNR) are usually sufficiently high that regularization can be achieved by a relatively simple and fast procedure, without actually changing the form of the function to be optimized. With experimental error considered to have Poisson distribution:

$$\chi^2 = \frac{1}{M} \cdot \sum_i^M \frac{1}{y_i} \cdot \left(y_i - \sum_k^N b_k \cdot \exp\left(-\frac{t_i}{\tau_k}\right)\right)^2, \qquad (8)$$

where y_i represents components of data vector and M is a total number of data points. Minimization of χ^2 should provide the best fit of the data vector and simultaneously give a set of coefficients b_k that represents an approximation of original phosphorescence intensity associated with the corresponding decay constants τ_k.

Physical principles require that the coefficients b_k can have only nonnegative values and, therefore, the search for χ^2 minimum has to be constrained. Thus, ESM method uses an extension of Marquardt-Levenberg nonlinear least-square algorithm to achieve such a restriction to positive values (James and Ware, 1986), and so solution is achieved iteratively, even though χ^2 is a linear function of parameters b_k. In our method of minimization, we made use of the fact that if χ^2 function is linearly dependent on parameter vector **b**, it

can be expressed as the following quadratic form:

$$\chi^2 = \frac{1}{2}(\mathbf{b}; \mathbf{Qb}) - (\mathbf{g}^0; \mathbf{b}) + \sum_i^M \frac{y_i^2}{\sigma_i^2}, \quad (9)$$

where $\mathbf{b}$ is parameter vector, $\mathbf{g}^0$ is anti-gradient vector calculated at the zero point, $\mathbf{Q}$ is Hessian (matrix of second partial derivatives), and y_i and σ_i are elements of the data vector and SDs for each data point, respectively. Parentheses denote scalar products. Considering Poisson distribution of the measurement errors, the constant term in Eq. 9 becomes the simple sum over the elements of the data vector and $\mathbf{g}^0$ and $\mathbf{Q}$ have components

$$g_j^0 = \frac{1}{M} \cdot \sum_i^M \exp\left(-\frac{t_i}{\tau_j}\right)$$
$$Q_{jk} = \frac{1}{M} \cdot \sum_i^M \frac{1}{y_i} \cdot \exp\left(-\frac{t_i}{\tau_j}\right) \cdot \exp\left(-\frac{t_i}{\tau_k}\right). \quad (10)$$

Minimization of χ^2 function, therefore, might be stated as maximization of the form

$$z = (\mathbf{g}^0; \mathbf{b}) - \tfrac{1}{2}(\mathbf{b}; \mathbf{Qb}), \quad (11)$$

subject to inequality constraints $b_k > 0$. Several algorithms have been suggested in the literature for solution of this problem (Houthakker, 1960; Wolfe, 1960; Shrager, 1972). We have chosen a quadratic programming algorithm proposed by Shrager, which appeared to be simple in implementation and very efficient. In this algorithm, only a finite number of steps is required to achieve optimal solution. The detailed description of the procedure is given in Shrager (1972), so here we will only point out a few major properties of the technique, which related to our particular problem.

Because of high redundancy of exponential basis and presence of noise in the data, the Hessian matrix is usually very close to singular. Because a major step in Shrager's algorithm is inversion of submatrices derived from the Hessian matrix, certain attention should be paid to singularity. We have used singular value decomposition (SVD) and subsequent analysis of singular values (Press et al., 1992) for matrix inversion, to ensure that no significant errors have been generated. In cases when too high singularity has been detected, a slight magnification of Hessian diagonal was introduced, followed by a Newton-type correction of the result. Shrager suggested a value of approximately 0.0001 for a magnification factor μ; however, by using double precision presentation of floating point numbers we have been able to use values normally lower than 10^{-7}. In fact, the degree of magnification necessary for each particular analysis depends upon the signal-to-noise ratio (SNR) of the data. We have tested a number of simulated decays with various levels of Poisson noise added and found that too low magnification usually results in poor fits and nonrandom residuals. Moreover, it normally leads to generation of additional peaks in the solution and, therefore, the magnification factor μ actually plays role of a smoothness regularizer in our algorithm. We have found that in the range of noise levels typically obtained in our experiments $\log(\mu)$ is proportional to $\log$(SNR), where SNR is determined as a ratio of signal at the beginning of the decay to the amplitude of noise at the baseline level (Stanley et al., 1993). For SNR levels usually obtained in phosphorescence measurements (see Results and Discussion), a value of magnification of about 10^{-8} can be set and then the LU (Lower-Upper) or Cholesky decompositions, which are much faster in execution then SVD algorithm, can be used for matrix inversion.

The solution obtained with suggested technique has the following important properties. (a) The shape matches the original distribution when the generated signal is noiseless. (b) It is smooth, which is assured by properly chosen magnification μ; (c) It only shows features if demanded by data as, for instance, MEM solution (Livesey and Brochon, 1987). (d) It is robust to noise, in the sense that decreasing of SNR leads to the predictable broadening of peaks and loss in resolution, but does not generate such artifacts as additional peaks, etc. (e) The shape of the solution is not dependent on the number of optimized parameters, and resolution ability improves with increasing number of basis terms. (f) Finally, no bias is introduced in the shape of recovered distribution, because initially all parameters are set to zero values, which is required by algorithm. As in regularized least-square solutions, solution found with this method cannot be easily proven to be uncorrelated, which is only true for the case of MEM (Livesey and Brochon, 1987). However, as it will be demonstrated below, recoveries of both synthetically simulated and *a priori* known experimentally modeled distributions are close enough to the originals to make the technique practically useful.

Of course, the main advantage of using Shrager's algorithm is its speed. Because the solution is achieved in the finite number of steps, unlike in iterative methods, and there is no need to compute either quadratic (Hessian matrix) or linear components (gradient vector) on each iteration, the actual time needed for calculations is limited by computing of the initial Hessian matrix. This is proportional to the number of points in the data vector and square of number of basis functions. The rest of the calculations are fast by comparison. Indeed, even if decay is presented in all lifetime interval $[\tau_{min}; \tau_{max}]$, then the longest step is just inversion of $N \times N$ matrix, where N is number of basis functions. If the required time is t s, then total time needed to complete the calculations is approximately $(t\sqrt{t})/3$ s. Thus, total computation time becomes longer with an increase in the number of exponentials with significant b_k values, but in reality once Hessian matrix was computed actual deconvolution process is practically instantaneous.

Finally, we would like to point out one very important, from our standpoint, property of the suggested algorithm. It can be easily shown that if noise in the data is not Poisson but normally distributed and no weighting has to be applied to χ^2 function, only the gradient, but not Hessian, is actually dependent on the data. This means that this matrix can be computed only once and stored in the file for all further

experiments that use the same basic set of functions and the frequency of digitization. In this case, deconvolution becomes fast enough to be implemented as a run time process. Obviously, all time domain kinetic measurements are limited to the case of Poisson distributed noise, and so the Hessian matrix has to be computed for each set of data. However, noise might be considered practically normally distributed for the case of frequency domain measurements with variable phase-shift and modulation (Lakowicz et al., 1984). Then this additional advantage of our algorithm can be effectively used.

MATERIALS AND METHODS

Materials

All solvents were obtained from Aldrich Chemical Co. (Milwaukee, WI). Tetrahydrofuran (THF), used in a preparation of solutions of phosphors, was distilled from $LiAlH_4$, degassed by a few freeze-pump-thaw cycles, and stored in vacuum over Na benzophenon ketyl. All other solvents have been used as purchased. Deionized and degassed water was used throughout.

Glucose, imidazole, Bovine serum albumin (BSA), catalase (bovine liver, H_2O_2:H_2O_2 oxidoreductase, E.C. 1.11.1.6), and glucose oxidase (type II, β-D-(+)glucose:O_2 oxidoreductase, E.C.1.1.3.4) were obtained from Sigma Chemical Co. (St. Louis, MO). Pd-*meso*-tetra (4-carboxyphenyl) porphyrin (PdTCPP) and Pd-*meso*-porphyrin (PdMP) were obtained from Porphyrin Products, Inc. (Logan, UT).

Nitrogen (N_2) and a mixture of nitrogen and oxygen containing 2.89% O_2 were purchased from Airco, Co. (Philadelphia, PA)

Instrumentation

UV-Visible spectra were recorded using a Beckman DU-64 spectrophotometer. Static phosphorescence spectral measurements were performed on an SPF-500C spectrofluorimeter (SLM Instruments, Inc., Urbana, IL). Time-correlated phosphorescence measurements were obtained with an OXYSPOT light-guide phosphorimeter (Medical Systems Corp., Greenvale, NY). This phosphorescence measurement system has been described in detail by Pawlowski and Wilson (1992). A 524 nm (25 nm width) interference filter and a 635 nm long pass filter (Shott, Inc., Milwaukee, WI) were used for filtering excitation and emitted light, respectively. Decays were collected using a 12 bit 1 MHz A/D converter (Metrabyte, DAS-50) mounted in a 386 16 MHz AT microcomputer and stored on the disk for further analysis. All calculations were performed on Gateway 2000 P5-60 MHz microcomputer system.

Preparation of samples and measurements

All samples for the phosphorescence measurements had approximately 10 μM concentrations of the phosphors. PdTCPP and PdMP were stored in concentrated DMF stock solutions in a dark room and transferred into the measurement cuvettes the day they were used. THF was vacuum-transferred to the sample cuvettes containing either solid porphyrins or small drops of stock solutions immediately before use and sealed in a vacuum. DMF samples were degassed by several freeze-pump-thaw cycles and sealed in a vacuum.

Binding of Pd porphyrins to BSA is described elsewhere (Vanderkooi et al., 1987). Water solutions of PdTCPP and PdMP bound to BSA were deoxygenated using catalytic amounts of glucose oxidase and catalase. Small amounts of the enzymes were added to the solutions of porphyrins in buffered media (10 mM MOPS, 10 mM KH_2PO_4, 10 mM Tris, and 120 mM NaCl; pH = 7.2) containing 0.020 to 0.1 M glucose, and the vials were immediately sealed.

Samples equilibrated with a nitrogen:oxygen gas mixture containing 2.89% O_2 were prepared by bubbling the mixture with gas until there was no further change in phosphorescence lifetime.

Phosphorescence measurements were made using a bifurcated lightguide, with a focusing lens on the end, which was placed against the side of the vial with sample. Samples with more than one "discrete component" were made by putting together a few thin cuvettes, each with its own sample, characterized by its own lifetime. Cuvettes were fixed one to each other by Scotch tape, and the lightguide end was fixed on the side of this construction.

Programming and computation

The simulation and deconvolution programs (Copyright, University of Pennsylvania) were written in C-language and compiled with Watcom 9.5 32-bit optimizing compiler. In all cases, double-precision presentation of floating point numbers has been used. The design matrix was composed of N single exponential terms, usually equally spaced in lifetime space, plus one constant term, representing the baseline. N varied from 80 to 300 in different numerical experiments and usually has been set at 200 for analysis of experimental data. In this software version, the design matrix is written directly into a memory and for a 200 exponential basis set and a data vector represented by 3000 points it requires 4.8 MB address space. The time needed for deconvolution of such a sample is approximately 120 s (200 exponential basis). Calculation time increases proportionally to the square of the number of basis functions. In all cases, a delay was introduced between the excitation flash and initiation of the data array (~30 μs), a delay comparable with that used when digitizing phosphorescence data with the phosphorimeter. Random Poisson distributed noise was superimposed on the data before analysis. The magnitude of noise has been measured as ratio of signal in the maximal channel to the average amplitude of noise of zero mean. This signal-to-noise ratio (SNR) varied from 4000 to 100 for different simulations. Data vectors consisting of 3000 data points, taken at 1-μs intervals, were used in most numerical experiments with simulated data. This number of data points matches 3 ms of data taken by the 1 MHz A/D board of the phosphorimeter typically used in phosphorescence measurement experiments, although other acquisition times and sampling frequencies can be used if necessary. Simulated decays were scaled to values of about 4000 at the first point, consistent with use of a 12 bit A/D board. Analysis of experimental curves always began by assuming a multiexponential distribution of lifetimes in a range of 0–1 ms, and then this range was narrowed if necessary. Goodness of fit was measured by the magnitude of weighted χ^2 and appearance of the plot of the residuals.

RESULTS AND DISCUSSION

Before applying a new computational tool to experimental data, one always should know exactly which limitations this tool has and be certain that it will not introduce bias in the calculated characteristics of the system. We focused, therefore, on the situations where the distributions of lifetimes were known a priori, and by the ability of the algorithm to recover these distributions we could judge its performance. Thus, we start the discussion from analyses of synthetically simulated decays. Here emphasis was on the examples characterized by different SNR values. Noise present in the data affects differently different computational algorithms, and each algorithm recovers one solution from the large set of feasible solutions satisfying data within the given noise level. That is why analysis of behavior of the method at various noise levels is critically important both for evaluation of this particular technique and for the comparison with other known algorithms.

Unfortunately, there are no cases known to date where continuous distributions of phosphorescence lifetimes with

different, known a priori shapes can be experimentally obtained. Therefore, we were limited only to computer simulation studies in this part of the paper. On the contrary, it was rather easy to make measurements in samples with discrete distributions of the lifetimes, and so these cases have been extensively investigated.

Efficiency of deconvolution in recovering simulated lifetime distributions

Fig. 1 shows the ability of the deconvolution to recover three exponential decays from a curve generated by combining components with lifetimes: 10, 200, and 650 μs. The data vectors were simulated as described in Materials and Methods. Noise of different magnitude has been added to the decays: SNR = 4000 (*a*), SNR = 800 (*b*), SNR = 100 (*c*). All recoveries were carried out with μ set at 10^{-7}. Deconvolution was into a set of 150 exponentials over the range 1–1000 μs. As shown in Fig. 1, in all cases recovery has been successful and at a satisfactory precision; however, slight broadening of the line corresponding to the longest lifetime component takes place for all signal-to-noise levels. At SNR = 800, a small additional peak appeared at 1000 μs and its amplitude increased with decrease of SNR (see Fig.1 *c*). The same effect was observed when recovery was done with Expectation Maximization (EM) and Regularized Least Squares (RLS) (Stanley et al., 1993), and that was attributed to the instability of the computational methods at high noise levels.

The ability of our deconvolution routine to recover discrete phosphorescence decays with not very different lifetimes is demonstrated in Fig. 2. The position of the shorter decay has been set at 100 μs, and the longer component was moved to 120 μs (*a*), 140 μs (*b*), and 170 μs (*c*), giving relative separation of the peaks, measured by $r = \tau_1/\tau_0$ of 1.2, 1.4, and 1.7, respectively. SNR and μ were set at 800 and 10^{-8}, respectively. Probe function consisting of 200 exponentials spaced in the range 0–500 μs was used for the deconvolution. Satisfactory resolution was obtained when decays were separated by about 10 units of the basis grid at this signal-to-noise, which is consistent with the resolution (9-grid-points separation) reported for EM and RLS.

The relative fraction of the phosphorescence originating from each of the participating components is indicated by the integral of respective peaks. The sum of areas of two separate peaks for $r = 1.7$ ($S = 8725$) approximately matches the area of signal obtained for the situation when lifetimes were not

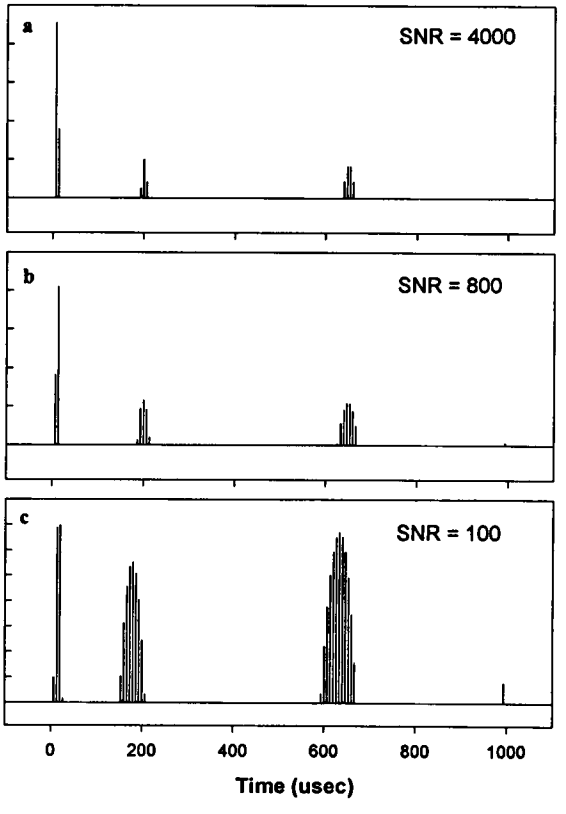

FIGURE 1 Deconvolutions of decays composed of three single exponentials with lifetimes: 10, 200, and 650 μs. Poisson noise was added to give SNR* values of 4000 (*a*), 800 (*b*), and 100 (*c*). 2000 data points were taken with frequency 600 kHz after delay of 30 μs. Signal level in maximal channel: 3996. Probe function: 150 terms evenly spaced in the range 1–1000 μs.
*SNR is defined as a ratio of data at the maximum of the decay to the average amplitude of noise (See Materials and Methods for details).

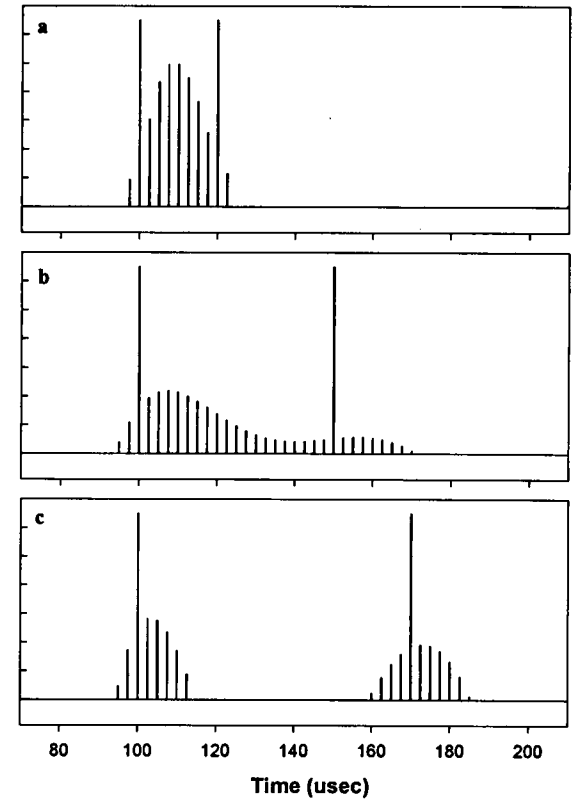

FIGURE 2 Recovery of two single exponentials with different separations in lifetime space. Positions of the original components (indicated with long vertical lines): (*a*) 100 and 120 μs (r = 1.2), (*b*) 100 and 140 μs (r = 1.4), and (*c*) 100 and 170 μs (r = 1.7). SNR = 800 for all cases. Data acquisition parameters: 1000 data points, 1 MHz frequency, delay 37 μs. Probe function: 200 terms in the range 0–500 μs.

resolved at all (r = 1.2) (S = 8549). Reconstruction of the decays at r = 1.4 demonstrates that the overall integral intensity of participating decays is also reproduced very well (S = 8632); however, the ratio of integrals is significantly weighted toward the shorter lifetime component.

The careful study of simulated continuous distributions of lifetimes is particularly important because these distributions are most representative of oxygen measurements in biological samples. In tissue, for example, oxygen is present in a wide range of concentrations and, therefore, the experimental curves are necessarily summations of a large number of exponentials. However, we know of no way to experimentally generate data with a known distribution of this type and have used, therefore, simulated distributions to test the deconvolution algorithm. Continuous distributions of the different shapes have been simulated and analyzed. Gaussian with a width at half-height σ = 150 μs and lifetime τ = 400 μs at the maximum amplitude was constructed as described in Materials and Methods, and one single exponential term imitating a residual of the excitation flash was added. Deconvolution was performed using a 200-exponential basis with μ set at 10^{-8}. Fig. 3 shows recoveries for SNR = 4000 (*a*), SNR = 1000 (*b*), and SNR = 400 (*c*). In each case, the decay of the flash lamp is readily separated from the distributions of phosphorescence. Increase in the noise level leads to attenuation of the wings of the distributions and broadening of recovered shapes. Estimated values for σs were 174 (*a*), 192 (*b*), and 212 (*c*) μs, respectively. In all three cases, deconvolution was performed using evenly spaced set of basis functions in lifetime space. Normal broadening of signals at longer lifetimes, which is caused by asymmetry of exponentials, leads to extension of the falling edges of the recovered Gaussians (first two cases). This effect would be eliminated if recovery were performed using a logarithmically spaced basis, but then data should also be presented using log (lifetime) scale. In the last case (*c*), however, the shape of the distribution shows a different asymmetry, and this is probably caused by the effect of the large noise (SNR = 400). As the result of such behavior of distribution wings, the peak positions are shifted toward the opposite directions: 391 (*a*); 374 (*b*), and 410 (*c*) μs, and so the weighted means tend to have a correct positions. Indeed, regular nonlinear fitting of the recovered distributions with Gaussian functions gave values 400, 392, and 403 μs for *a*, *b*, and *c*, respectively. All three of the latter values are close to the original Gaussian mean. In general, the observation that the distributions shift toward shorter lifetimes at higher noise levels has been observed for all of the simulated systems. The typical SNR, obtained for experimentally measured curves, is greater than about 700 where this effect is relatively low.

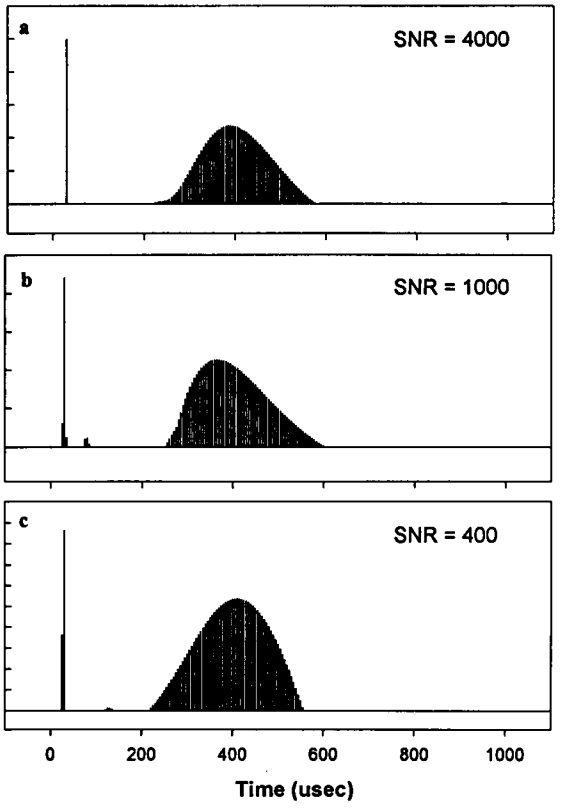

FIGURE 3 Reconstruction of Gaussian convoluted from 500 exponentials: τ = 400 μs, σ = 150 μs. The shortest lifetime component represents the flash lamp decay at 20 μs. Poisson noise has been added to give SNR values of 4000 (*a*), 1000 (*b*), 400 (*c*). Data acquisition parameters: 1800 data points, 800 kHz frequency, delay 20 μs. Probe function: 200 terms from 1 to 1000 μs. Positions (τs) and widths at half-height (σs) of the recovered distributions in microseconds are: (*a*) 391, 174; (*b*) 374, 192; (*c*) 410, 212, respectively. The maxima found by fitting the distributions with Gaussian functions were 400, 392, and 403 μs for *a*, *b*, and *c*, respectively.

Bimodal distributions were constructed from two Gaussians ($\sigma_1 = \sigma_2$ = 70 μs) separated by 100, 150, and 250 μs in lifetime space. The original distributions (simulated) of lifetimes appear in the left column on Fig. 4 (a1, a2, a3). These distributions were simulated using two different noise levels, and results of recoveries are shown in two columns separately: SNR = 800 (b1, b2, b3) and SNR = 400 (c1, c2, c3). As expected, the ability of the algorithm to resolve the Gaussians decreases with decrease in signal-to-noise, and significant broadening of longer lifetime peaks takes place when the SNR is 100. Obtained values for width at half-height of the peaks are: 81, 103 (b3) and 137, 192 (c3). The positions of Gaussians were recovered with much better precision and always lay within 15–25 μs of the original mean lifetimes. As shown in the figure, our method allows only partial resolution of the maxima when they separated by 1.5σ (Fig. 4 *a*), but they are well resolved when separation is approximately 4σ. Dependent on the signal-to-noise, both the leading and falling edges of distributions were attenuated in a manner similar to that described for unimodal distributions.

Experimental data collection and analyses

The ability of the technique to recover the shapes of experimentally obtained distributions was checked using phosphorescent samples based on two phosphors used for oxygen measurements: Pd TCPP and PdMP. The phosphors were

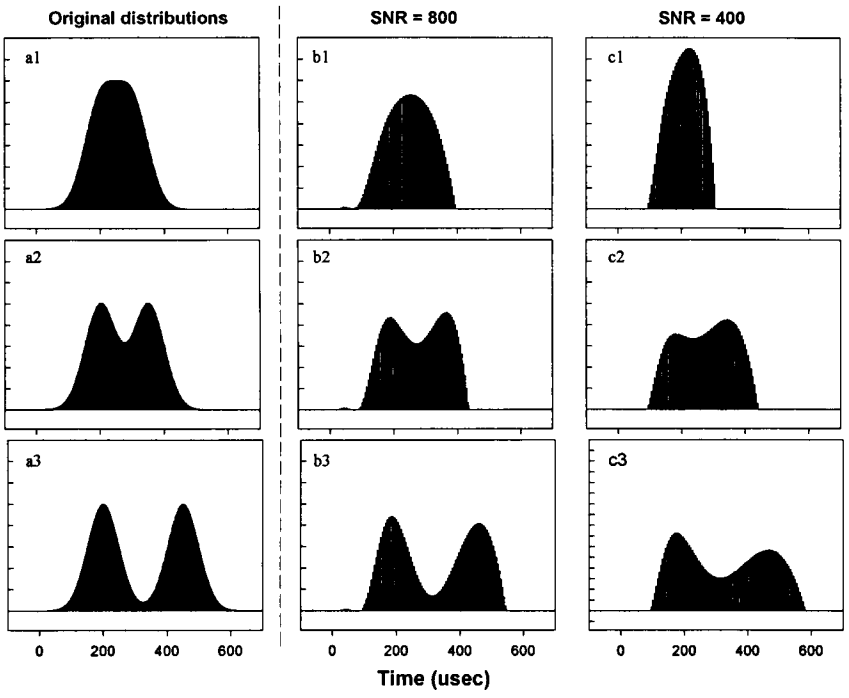

FIGURE 4 Recovery of decays consisting of two Gaussian distributions of exponentials. The distributions (a1, a2, a3) were constructed from two Gaussians ($\sigma_1 = \sigma_2 = 70$ μs) separated by 100, 150, and 250 μs, respectively. Decays consist of 1800 data points taken with 800 kHz frequency, delay 20 μs. Poisson noise to give SNR values of 800 (b1, b2, b3) and 400 (c1, c2, c3) has been added. Probe function: 150 terms in the range of 0–600 μs.

excited at the Q-band (524 ± 18 nm interference filter), and emission was measured with a 635 nm longpass filter.

The decay of the flash lamp has been analyzed (Fig. 5). As expected, it shows a strong maximum at 7 μs (96.8%) but it also shows small additional components at 18 μs (3%) and 95 μs (<0.3%). The smallest component was found to appear in the range 50–100 μs for different sets of measured flash decays. The exact position depends on the relative intensity of the measured signal. This behavior can be attributed to the nonexponential form of the flash lamp decay. The lifetimes of practical interest for measuring the oxygen pressure in biological systems lie in the range 40–1000 μs, which is well separated from the main flash lamp component. Considering that phosphorescence is usually at least 100–200 times higher in intensity than small components of the flash decay, the distortion introduced by the latter is generally negligible.

Typical decay curves collected from the experimental systems are presented in Fig. 6. The insert shows the tail of the decay *b* after subtraction of the first order regression line, to demonstrate the noise level. The maximal amplitude of noise in the real data after averaging of 100 repetitive flashes is approximately 5 units. This corresponds to the SNR of 800 (as determined in Materials and Methods), considering that maximal amplitude of signal is about 4000. The average SNR value measured for experimentally obtained curves lies in the range of 700–900, and so the value of the magnification factor μ has been set at 10^{-8} for further calculations. The lower plots (Fig. 6) show the residuals after fitting the decay *b* and corresponding simulated decay with the SNR set at 800. Both residuals have similar appearances and amplitudes, which indicates correct recovery for a given SNR value. Fig. 7 presents the result of analyses of three experimental measurements of phosphorescence. In each case, recovery shows good separation from the flash lamp component and slight broadening of the peaks with a longer lifetimes, an effect also noticed during the analyzes of simulated curves. This is caused by nonproportional distortion, caused by introducing the magnification factor into the Hessian matrix. Table 1 presents lifetime analysis for different samples.

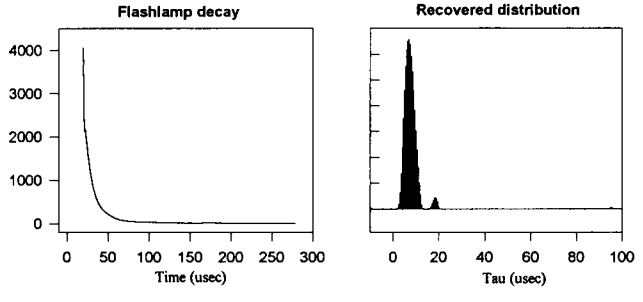

FIGURE 5 Reconstruction of the lifetime distribution associated with the flash lamp and detection electronics. Data: 278 points, 1 MHz frequency, A/D delay 12 μs. Probe function: 100 terms in the range 0–100 μs.

Solutions of Pd-porphyrins, taken at sufficiently low concentrations, should show single exponential decay of phosphorescence. Therefore, ordinary linear fitting of the *log* intensity can be employed for the data analysis. It should be pointed out, however, that the selected optical filters did not completely exclude flash lamp decay from the phosphorescence signal. Depending on the extent of its contribution, residual lamp signal might affect the results of single exponential fitting. The lifetimes obtained by fit to a single exponential are also presented in Table 1. They always show relatively small (about 15–25 μs) shift to shorter lifetimes, partly because of contribution by the flash lamp. In general,

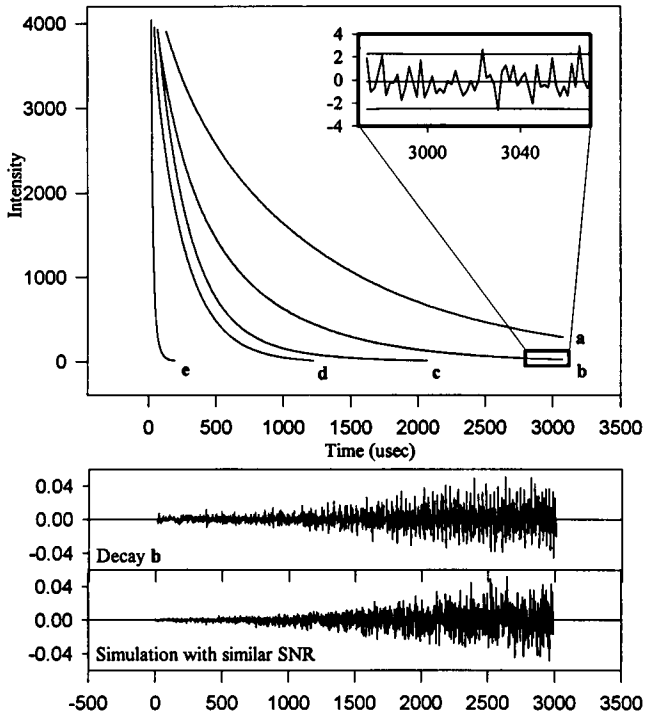

FIGURE 6 Typical decays collected from phosphorescent samples of Pd-porphyrins. (*a*) PdMP, deoxygenated water solution with BSA added. (*b*) PdTCPP, deoxygenated water solution with BSA added. (*c*) Mixed decay from samples *b* and *d*. (*d*) PdTCPP in DMF, degassed; (*c*) PdTCPP water solution with BSA at air saturation. Inset presents a small part of the decay *b* and shows that SNR characterizing this experimental data set is close to 800. Plot of weighted residuals is shown below. Lowest graph presents residuals after the recovery of corresponding simulated decay, generated with SNR also equal 800.

lifetimes obtained by deconvolution should better represent the real characteristics of the systems. Thus, it is desirable to use τ_0 values for phosphorescence probes obtained using the same method as for oxygen measurement.

Pd-porphyrins bound to serum albumin are most often used to measure oxygen. The phosphorescence decays of both porphyrin compounds in homogeneous solution with albumin were found to be very close to pure single exponentials as evidenced by very narrow distributions after the decays were deconvoluted. This is consistent with the probes binding to a single site on the large BSA molecule. The presence of more than one site with different binding properties would make the probes' behavior more like that reported recently for the luminescence behavior of Re complexes incorporated into polymers (Sacksteder et al., 1993). The observed single exponential decay of phosphorescence of the Pd-porphyrins bound to albumin is of great practical importance when these probes are used for reconstruction of the oxygen distributions in tissue through analysis of the distribution of lifetimes.

The distributions of phosphorescent decays collected from "heterogeneous" samples are presented in Fig. 8. The first graph (1) belongs to the system where the data for two independent decays was collected from two samples simultaneously (see Materials and Methods for details). Both samples, deoxygenated DMF and aqueous solution with BSA, of PdTCPP were analyzed separately and gave lifetimes of 223 and 700 μs, respectively. Deconvolution of the data from the mixed samples showed recovery of the two independent decay constants with values of 200 and 687 μs. Analysis of the simulated curves composed of two exponentials with these given lifetimes, flash lamp and Poisson noise of the same average amplitude showed that positions of peaks were recovered with excellent precision. We suggest, therefore, that the alterations in peak position of the components of experimentally convoluted curves is the result of some nonstatistical noise present in the data.

A similar effect was noticed when the phosphorescence decay was collected from a solution containing both porphyrins (PdTCPP and PdMP) in the presence of an excess of BSA, and the solution deoxygenated before the measurements (Fig. 8; graph 2). The lifetime distributions recovered from the measurements of individual solutions have lifetimes 665 μs (*a*) and 1183 μs (*b*). Deconvolution of phosphorescence decays from solutions containing both porphyrins gave phosphorescence lifetimes corresponding to PdTCPP (611 μs) and PdMP (1060 μs) that were well resolved, although shifted by 55 and 123 μs, respectively. This shift might be caused by some interaction between probe mol-

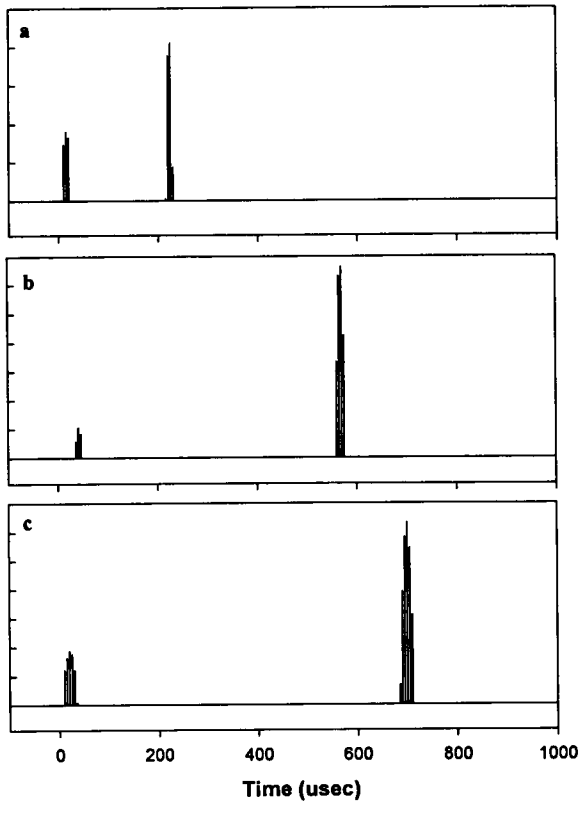

FIGURE 7 Results of analyzes of three experimental curves. (*a*) PdTCPP in DMF, degassed. (*b*) PdMP in DMF, degassed. (*c*) PdTCPP and BSA in water, deoxygenated. Decays collected with frequency 600 kHz, A/D delays: 42, 50, and 102 μs, respectively. Probe function: 200 terms in 0–1000 μs range.

TABLE 1 Phosphorescent lifetimes for homogeneous samples

Sample	Solvent	State of oxygenation	Sampling frequency (kHz) and A/D delay (μs)	Lifetime obtained from single exponential fitting (μs)	Results of the deconvolution analysis (μs)
PdTCPP*	DMF	deox.¶	600, 42	195	223
PdTCPP	THF	deox.	750, 37	434	465
PdTCPP	H_2O	deox.	1000, 34	477	522
PdTCPP + BSA‡	H_2O	deox.	600, 35	670	700
PdTCPP + BSA	H_2O	2.89% O_2‖	1000, 34	139	157
PdTCPP + BSA	H_2O	air satur.**	1000, 20	29	48
PdMP§	DMF	deox.	600, 52	540	568
PdMP	THF	deox.	600, 67	671	722
PdMP	H_2O	deox.	600, 81	811	975
PdMP + BSA	H_2O	deox.	300, 19	1108	1162
PdMP + BSA	H_2O	2.89% O_2	1000, 32	239	261
PdMP + BSA	H_2O	air satur.	600, 21	50	66

* Pd *meso*-tertacarboxyphenyl porphyrin.
‡ Bovine serum albumin ("+" denotes binding of the corresponding porphyrin to the protein molecule).
§ Pd *meso*-porphyrin.
¶ Samples were deoxygenated according to the procedures described in Materials and Methods.
‖ Samples were equilibrated with gas mixture, containing 2.89% oxygen.
** Samples were equilibrated with atmospheric air.

ecules, such as slight quenching by the ground state molecules at the combined concentrations, or even the presence of a trace of O_2.

The measured phosphorescence decays from six different samples were added together, and the resulting decay was analyzed. Aquisitions of up to 250 decays for each sample independently have been used for this experiment, so an SNR of 2000 has been achieved. The samples, with the lifetimes measured before mixing in parentheses, were: PdTCPP bound to BSA at air saturation (37 μs), PdMP bound to BSA at air saturation (66 μs), PdTCPP bound to BSA at 2.89% oxygen (157 μs), PdTCPP in DMF (465 μs), and PdMP solutions in DMF and THF (586 and 722 μs, respectively). The results are shown in Fig. 9. The recovered lifetimes were 38, 67, 160, 460, and 666 μs and indicate that positions of the decays are reproduced with very good accuracy; however, longer lifetime components became significantly broader. In fact, the components with lifetimes of 586 and 722 μs were not resolved but appear as one broad signal covering the region of the original decays. Together these components constitute only about 12% of the total phosphorescence signal.

CONCLUSION

Analyses of synthetically constructed and experimentally measured phosphorescence decays illustrate that the deconvolution algorithm described here can very efficiently recover distributions of lifetimes from experimental data. Because constrained global minimization of χ^2 function was used, the locus of the solution for the tested algorithm theoretically matches the locus ESM. Distortion of the lifetime distributions, introduced by the magnification parameter μ, makes it slightly different. We have found, however, that constrained Marquardt-Levenberg algorithm applied to the reconstruction of phosphorescence lifetime distributions

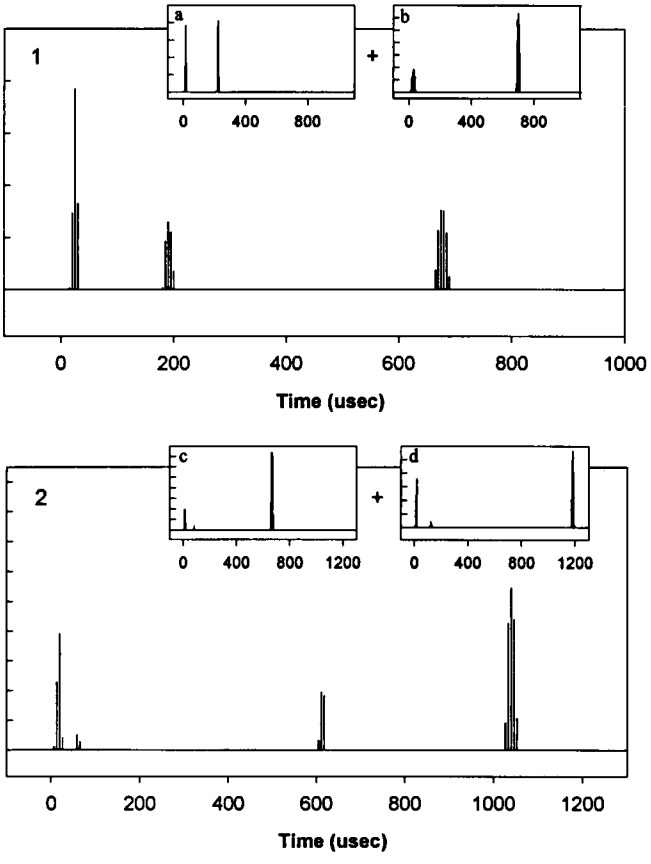

FIGURE 8 Analysis of the decays collected from two homogeneous samples simultaneously (1), and from homogeneous solution of two different porphyrins (2). (1) Data acquisition: frequency 600 kHz, A/D delay 37 μs. Probe function: 200 terms in the 0–1000 μs range. Recovered lifetimes: τ_1 = 200 μs and τ_2 = 687 μs. Small graphs show distributions recovered from independently collected decays with lifetimes 223 μs (*a*) and 700 μs (*b*). (2) Data acquisition: frequency 600 kHz, A/D delay 42 μs. Probe function: 200 terms in the 0–1300 μs range. Recovered lifetimes: τ_1 = 610 μs and τ_2 = 1060 μs. Individual peaks: 665 μs (*c*) and 1183 μs (*d*).

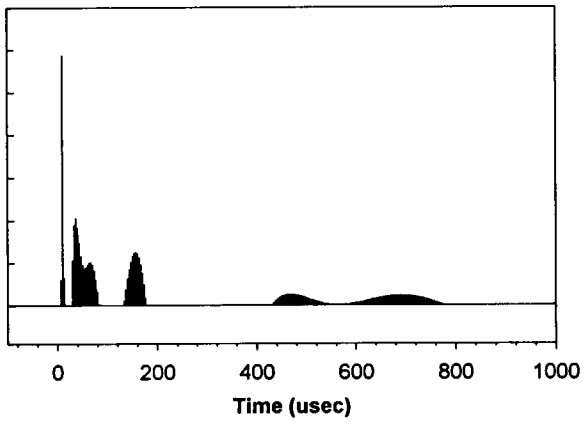

FIGURE 9 Extraction of separate decays from a data vector constructed by summing experimentally obtained curves. Participating decays: PdTCPP bound to BSA at air saturation (37 μs), PdMP bound to BSA at air saturation (66 μs), PdTCPP bound to BSA at 2.89% oxygen (157 μs), PdTCPP in DMF (465 μs), and PdMP solutions in DMF and THF (586 and 722 μs, respectively) were added together.

(Vinogradov and Wilson, 1993) gives results similar to those obtained with this technique, but was much less robust to noise. In addition, the present algorithm is much faster in execution and simpler to code.

As has been shown in examples in the text, recovery of distributions of lifetimes from experimentally obtained data can be performed with reasonable accuracy. However, attention still has to be paid to the noise level, because high noise can significantly affect the broadness of the recovered peaks.

In general, applicability of our deconvolution algorithms to analysis of phosphorescence decay data appears well justified and offers an important advance in analysis of data from systems with phosphors in heterogeneous environments. An important application of suggested method is recovery of oxygen distributions in tissue.

S. A. Vinogradov thanks Dr. M. S. Topaler for helpful discussion.
This work was supported by grant 2R44-NS30265 and PO1-CA56679 from National Institutes of Health.

REFERENCES

Alcala, J. R., C. Yu, and G. J. Yeh. 1993. Digital phosphorimeter with frequency domain signal processing: application to real-time fiber-optic oxygen sensing. *Rev. Sci. Instrum.* 64:1554–1560.

Baron, A. E., J. D. S. Danielson, M. Gouterman, J. R. Wan, J. B. Callis, and B. McLachlan. 1993. Submillisecond response times of oxygen-quenched luminescent coatings. *Rev. Sci. Instrum.* 64:3394–3402.

Carraway, E. R., J. N. Demas, and B. A. DeGraff. 1991a. Photophysics and oxygen quenching of transition-metal complexes on fumed silica. *Langmuir.* 7:2991–2998.

Carraway, E. R., J. N. Demas, and B. A. DeGraff. 1991b. Luminescence quenching mechanism for microheterogeneous systems. *Anal. Chem.* 63: 332–336.

Eastwood, D., and M. Gouterman. 1970. Porphyrins. XVIII. Luminescence of (Co), (Ni), Pd, Pt complexes. *J. Mol. Spectrosc.* 35:359–375.

Gardner, D. G., J. C. Gardner, and W. W. Meinke. 1959. Method for the analysis of multicomponent exponential decay curves. *J. Chem. Phys.* 31:978–986.

Gehlen, M. H., and F. C. Schryver. 1993. Time-resolved fluorescence quenching in micellar assemblies. *Chem. Rev.* 93:199–221.

Houthakker, H. S. 1960. The capacity method of quadratic programming. *Econometrica.* 28:62–87.

James, D. R., and W. R. Ware. 1985. A fallacy in the interpretation of fluorescence decay parameters. *Chem. Phys. Lett.* 120:455–459.

James, D. R., and W. R. Ware. 1986. Recovery of underlying distributions of lifetimes from fluorescence decay data. *Chem. Phys. Lett.* 126:7–11.

Lacowicz, J. R., G. Laczko, H. Cherek, E. Gratton, and M. Limkeman. 1984. Analysis of fluorescence decay kinetics from variable-frequency phase shift and modulation data. *Biophys. J.* 46:463–477.

Livesey, A. K., and J. C. Brochon. 1987. Analyzing the distribution of decay constants in pulse-fluorimetry using maximum entropy method. *Biophys. J.* 52:693–706.

Pawlowski, M., and D. F. Wilson. 1992. Monitoring of the oxygen pressure in the blood of live animals using the oxygen dependent quenching of phosphorescence. *Adv. Exp. Med. Biol.* 316:179–185.

Pekcan, O. 1992. Inverted Klafter-Blumen equation for fractal analysis in particles with interpenetrating network morphology. *Chem. Phys. Lett.* 198:20–24.

Press, W. H., S. A. Teukolsky, W. T. Vetterling, and B. P. Flannerly. 1992. Numerical Recipes in C. The Art of Scientific Computing, 2nd ed. Cambridge University Press. 994 pp.

Provencher, S. W. 1976a. An eigenfunction expansion method for the analysis of exponential decay curves. *J. Chem. Phys.* 64:2772–2777.

Provencher, S. W. 1976b. A Fourier method for the analysis of exponential decay curves. *Biophys. J.* 16:27–41.

Provencher, S. W. 1982a. A constrained regularization method for inverting data represented by linear algebraic or integral equations. *Comput. Phys. Commun.* 27:213–227.

Provencher, S. W. 1982b. CONTIN: a general purpose constrained regularization program for inverting noisy linear algebraic and integral equations. *Comput. Phys. Commun.* 27:229–242.

Robiolio, M., W. R. Rumsey, and D. F. Wilson. 1989. Oxygen diffusion and mitochondrial respiration in neuroblastoma cells. *Am. J. Physiol.* 256: C1207–C1213.

Rumsey, W. L., J. M. Vanderkooi, and D. F. Wilson. 1988. Imaging of phosphorescence: a novel method for measuring the distribution of oxygen in perfused tissue. *Science.* 241:1649–1651.

Sacksteder, L., J. N. Demas, and B. A. DeGraff. 1993. Design of oxygen sensors based on quenching of luminescent metal complexes: effect of ligand size on heterogeneity. *Anal. Chem.* 65:3480–3483.

Siemiarczuk, A., B. D. Wagner, and W. R. Ware. 1990. Comparison of the Maximum Entropy Method and Exponential Series Method for the recovery of distributions of lifetimes from fluorescence lifetime data. *J. Phys. Chem.* 94:1661–1666.

Siemiarczuk, A., and W. R. Ware. 1989. A novel approach to analysis of pyrene fluorescence decays in sodium dodecylsulfate micelles in the presence of Cu^{2+} ions based on the Maximum Enthropy Method. *Chem. Phys. Lett.* 160:285–290.

Siemiarczuk, A., and W. R. Ware. 1990. Pyrene lifetime broadening in SDS micelles. *Chem. Phys. Lett.* 167:263*a*. (Abstr.)

Siemiarczuk, A., W. R. Ware, and Y. S. Liu. 1993. A novel method for determining size distributions in polydisperse micelle systems based on the recovery of fluorescence lifetime distributions. *J. Phys. Chem.* 97: 8082–8091.

Shonat, R. D., D. F. Wilson, C. E. Riva, and M. Pawlowski. 1992. Oxygen distribution in the retinal and choroidal vessels of the cat as measured by a new phosphorescence imaging method. *Appl. Opt.* 31:3711–3718.

Shrager, R. I. 1970. Nonlinear regression with linear constraints: an extension magnified diagonal method. *J. Assoc. Comp. Machin.* 17: 446–452.

Shrager, R. I. 1972. Quadratic programming for nonlinear regression. *Comm. ACM.* 15:41–45.

Skilling, J., and R. K. Bryan. 1984. Maximum entropy image reconstruction: general algorithm. *Mon. Not. R. Astron. Soc.* 211:111*a*. (Abstr.)

Stanley, B. J., S. E. Bialkowski, and D. B. Marshall. 1993. Analysis of 1st-order rate-constant spectra with regularized least-squares and Expectation Maximization. 1. Theory and numerical characterization. *Anal. Chem.* 65:259–267.

Vanderkooi, J. M., G. Maniara, T. J. Green, and D. F. Wilson. 1987. An optical method for measurement of dioxygen concentration

based on quenching of phosphorescence. *J. Biol. Chem.* 262: 5476–5482.

Ware, R. 1991. Recovery of fluorescence lifetime distributions in heterogeneous systems. *In* Photochemistry in Organized and Constrained Media. V. Ramamurthy, editor. VCH Publishers, New York. 563–602.

Ware, W. R., L. J. Doemeny, and T. L. Nemzek. 1973. Deconvolution of fluorescence and phosphorescence decay curves. A least square method. *J. Chem. Phys.* 77:2038–2048.

Wilson, D. F., W. L. Rumsey, T. J. Green, and J. M. Vanderkooi. 1988. The oxygen dependence of mitochondrial oxidative phosphorylation measured by a new optical method for measuring oxygen. *J. Biol. Chem.* 263:2712–2718.

Wilson, D. F., and S. A. Vinogradov. 1993. Recent advances in oxygen measurements using phosphorescence quenching. *Adv. Exp. Med. Biol.* In press.

Vinogradov, S. A., and D. F. Wilson. 1993. Recovery of oxygen distributions in tissue from phosphorescence decay data. *Adv. Exp. Med. Biol.* In press.

Wolfe, P. 1959. The simplex method for quadratic programming. *Econometrica.* 27:382–398.